

# **SARS-CoV-2 exhibits intra-host genomic plasticity and low-frequency polymorphic quasispecies**

Timokratis Karamitros<sup>1#</sup>, Gethsimani Papadopoulou<sup>1</sup>, Maria Bousali<sup>1</sup>, Anastasios Mexias<sup>1</sup>, Sotiris Tsiodras<sup>2</sup>, Andreas Mentis<sup>3</sup>

1. Unit of Bioinformatics and Applied Genomics, Department of Microbiology, Hellenic Pasteur Institute, Athens, Greece
2. 4<sup>th</sup> Academic Department of Medicine, National and Kapodistrian University of Athens, Medical School, Athens, Greece.
3. Public Health Laboratories, Department of Microbiology, Hellenic Pasteur Institute, Athens, Greece

#To whom correspondence should be addressed:

Dr. Timokratis Karamitros

Researcher

Unit of Bioinformatics and Applied Genomics

Department of Microbiology

Hellenic Pasteur Institute

127 Vas. Sophias avenue

11521, Athens, Greece

m: tkaram@pasteur.gr

t: +30 2106478-871, -874

Word Count: 2597

## ABSTRACT

In December 2019, an outbreak of atypical pneumonia (Coronavirus disease 2019 - COVID-19) associated with a novel coronavirus (SARS-CoV-2) was reported in Wuhan city, Hubei province, China. The outbreak was traced to a seafood wholesale market and human to human transmission was confirmed. The rapid spread and the death toll of the new epidemic warrants immediate intervention. The intra-host genomic variability of SARS-CoV-2 plays a pivotal role in the development of effective antiviral agents and vaccines, but also in the design of accurate diagnostics.

We analyzed NGS data derived from clinical samples of three Chinese patients infected with SARS-CoV-2, in order to identify small- and large-scale intra-host variations in the viral genome. We identified tens of low- or higher- frequency single nucleotide variations (SNVs) with variable density across the viral genome, affecting 7 out of 10 protein-coding viral genes. The majority of these SNVs corresponded to missense changes. The annotation of the identified SNVs but also of all currently circulating strain variations revealed colocalization of intra-host but also strain specific SNVs with primers and probes currently used in molecular diagnostics assays. Moreover, we de-novo assembled the viral genome, in order to isolate and validate intra-host structural variations and recombination breakpoints. The bioinformatics analysis disclosed genomic rearrangements over poly-A / poly-U regions located in ORF1ab and spike (S) gene, including a potential recombination hot-spot within S gene.

Our results highlight the intra-host genomic diversity and plasticity of SARS-CoV-2, pointing out genomic regions that are prone to alterations. The isolated SNVs and genomic rearrangements, reflect the intra-patient capacity of the polymorphic quasispecies, which may arise rapidly during the outbreak, allowing immunological escape of the virus, offering resistance to anti-viral drugs and affecting the sensitivity of the molecular diagnostics assays.

**KEYWORDS**

SARS-CoV-2, COVID-19, intra-host variability, quasispecies, genomic recombination, Wuhan seafood market epidemic

## INTRODUCTION

Coronaviruses (CoVs), considered to be the largest group of viruses, belong to the *Nidovirales* order, *Coronaviridae* family and *Coronavirinae* subfamily, which is further subdivided into four genera, the alpha- and betacoronaviruses, which infect mammalian species and gamma- and deltacoronaviruses infecting mainly birds [1], [2]. Small mammals (mice, dogs, cats) serve as reservoirs for HCoVs, with significant diversity seen in bats, which are considered to be primordial hosts of HCoVs [3]. On the contrary, peridomestic animals are usually intermediate hosts, who enable long-term establishment of endemicity of the viruses, facilitating mutations and recombination events [1], [4].

Until 2002, minor consideration was given to HCoVs, as they were associated with mild-to-severe disease phenotypes in immunocompetent people [3]–[5]. In 2002, the beginning of severe acute respiratory syndrome (SARS) outbreak took place [6]. In 2005, after the discovery of SARS-CoV-related viruses in horseshoe bats (*Rhinolophus*), palm civets were suggested as intermediate hosts, and bats as primordial hosts of the virus [6], [7]. In 2012, the emerging Middle East respiratory syndrome coronavirus (MERS-CoV) caused an outbreak in Saudi Arabia, which affected both camels and humans (44% mortality).

On December 31<sup>st</sup> – 2019, a novel Coronavirus (SARS-CoV-2) was first reported from the city of Wuhan, Hubei province in China, causing severe infection of the respiratory tract in humans, after the identification of a group of similar cases of patients with pneumonia of unknown etiology [8] (<https://www.who.int/emergencies/diseases/novel-coronavirus-2019>). Similarly to SARS, epidemiological links between the majority of 2019-nCoV cases and Huanan South China Seafood Market, a live-animal market, have been reported. A total of 76,775 confirmed cases of “Coronavirus Disease 2019” (COVID-19) were reported up to February 21<sup>st</sup> 2020, from which 2,247 died and 18,855 recovered. Notably, 75,447 of the confirmed cases were reported in China (<https://www.qisaid.org/epiflu-applications/global-cases-betacov/>).

The size of the ssRNA genome of SARS-CoV-2 is 29,891 nucleotides, it encodes 9860 amino acids and is characterized by nucleotide identity of ~ 89% with bat SARS-related-CoV

SL-ZXC21 and ~ 82% with human SARS-CoVs BJ01 2003 and Tor2 [9]. CoVs are enveloped positive-sense RNA viruses, which are characterized by a very large non-segmented RNA genome (26 to 32kb length), ready to be translated [2], [5]. The genes arrangement on the SARS-CoV-2 genome is: 5'UTR -replicase (ORF1/ab) -Spike (S) -ORF3a -Envelope (E) - Membrane (M) -ORF6 -ORF7a -ORF8 -Nucleocapsid (N) ORF10 -3'UTR [9]. The main difference between SARS-CoV-2 and SARS-CoV is in ORF3b, ORF8 and Spike.

Intra host variability of pathogenic viruses and bacteria represents a significant barrier in the control of infectious diseases. In viral infections, this variation emerges from genomic phenomena taking place during error-prone replication, ending up to multiple circulating quasispecies of low or higher frequency [10], [11]. These variants, in combination with the genetic profile of the host, can potentially influence the natural history of the infection, the viral phenotype, but also the sensitivity of molecular and serological diagnostics assays [12], [13]. Importantly, intra-host genomic variability leads to antigenic variability, which is of higher importance, especially for pathogens that fail to elicit long-lasting immunity in their hosts, and remains a major contributor to the complexity of vaccine design [14], [15]. To date, there are no clinically approved vaccines available for protection of general population from SARS- and MERS-CoV infections as there is no effective vaccine to induce robust cell mediated and humoral immune responses [16], [17].

Here, we explore intra-host genomic variants and low-frequency polymorphic quasispecies in Next Generation Sequencing (NGS) data derived from patients infected by SARS-CoV-2. Our analyses provide insights into the intra-patient pool of viral genomes, identify the frequency levels of rare variants and highlight variable genomic regions and a potential recombination hot-spot within S gene. Intra-host genomic variability is critical for the development of novel drugs and vaccines, which are of urgent necessity, towards the containment of this newly emerging epidemic.

## MATERIALS AND METHODS

In this study we analysed NGS data derived from clinical specimens (oral swabs) from three Chinese patients infected by SARS-CoV-2 (SRA projects PRJNA601736 and PRJNA603194). We aligned the raw read data on reference strain MN975262.1 using bowtie2 [18], after quality check with FastQC ([www.bioinformatics.bbsrc.ac.uk/projects/fastqc](http://www.bioinformatics.bbsrc.ac.uk/projects/fastqc)). The resulting alignments were visualized with the *Integrated Genomics Viewer* (IGV) [19]. After removing PCR duplicates, SNVs were called with a Bonferroni-corrected  $P$ -value threshold of 0.05 using *samtools* [20] and *LoFreq* [21]. Variants supported by absolute read concordance (>98%) were filtered-out from intra-host variant frequency calculations. We annotated the variations to the reference strain using snpEff [22], SNVs effects were further filtered with snpSift [23] and we estimated the average mutation rate per gene across the viral genome using R scripts. We compared the localization of the intra-host SNVs with all available SNVs observed at population level up to February 18<sup>th</sup> 2020 (retrieved from [www.GISAID.org](http://www.GISAID.org)). We also compared all intra-host and population level SNPs with all primers and probes coordinates to investigate for potential interferences with currently available molecular diagnostic assays [24]([www.who.int/docs/default-source/coronaviruse/peiris-protocol-16-1-20.pdf](http://www.who.int/docs/default-source/coronaviruse/peiris-protocol-16-1-20.pdf)).

To investigate intra-host genomic rearrangements, we performed *de novo* assembly of the SARS-CoV-2 genomes using Spades [25], and the resulting contigs were analyzed with BLAST [26] and confirmed by remapping of the raw reads. Smaller contigs (<200 bp) were elongated where possible, after pair-wise realignment of the corresponding mapped reads. Basic computations and visualizations we implemented in R programming language R version 3.6.2, using in-house scripts. The secondary structures of the genomic regions surrounding the recombination breakpoints was predicted using RNAfold [27].

## RESULTS

The mapping assembly of the viral genome was almost complete for all samples. The genome coverage and the average read depth across the genome was 99.99% and 133.5x for sample SRR10903401, 99.99% and 522.5x for sample SRR10903402, and 99.94%, and 598.2x for sample SRR10971381, respectively. The alignment statistics for all samples are summarized in **Suppl.Table 1**.

In all cases we isolated the same 5 SNVs with 98-100% read concordance, thus in total divergence with the reference strain (MN975262.1), which were excluded from the downstream analysis. For sample SRR10903401 we isolated 34 lower frequency SNVs in total. Of these, 33 were present with frequencies ranking between 2 and 15%, while only one was present in 40% of the intra-host viral population. The sequencing depth, which is also evaluated during the SNV calling by the LoFreq algorithm, ranked between 39x and 290x at the corresponding SNV positions. The sequencing depth of sample SRR10903402 at the polymorphic positions was substantially higher (103x – 1137x), allowing the isolation of 55 SNVs with frequencies distributed between 0.9% and 14%. The depth over the polymorphic positions of sample SRR10971381 was between 159x – 1872x, allowing the isolation of 10 intra-host SNVs, with frequencies 1.1% - 6.8% (**Figure 1.A, Suppl.Table 2**).

Intra-host variants were distributed across 7 out of the 10 protein-coding genes of the viral genome, namely ORF1ab, S, ORF3a, ORF6, ORF7a, ORF8 and N. After normalising for the gene length (variants / kb-gene-length – “v/kbgl”), the higher density was observed in the small ORF6 (16.21 v/kbgl), followed by ORF8 (8.21 v/kbgl), N (4.76 v/kbgl), S (4.18 v/kbgl), ORF1ab (3.47 v/kbgl), ORF7a (2.73 v/kbgl) and ORF3a (1.21 v/kbgl). Interestingly, the majority of the SNPs corresponded to missense changes (leading to amino-acid change) compared to synonymous changes (72 vs. 29 respectively, ratio 2.48:1) (**Table 1**). The average intra-host variant frequency did not differ substantially either between missense and synonymous polymorphisms (**Figure 1.C**), neither between their hosting genes (**Figure 1.D**). We did not detect any small-scale insertions or deletions in the samples (**Suppl. Table 2**).

The comparison of all SNVs (intra-host and population level) with the genomic targets of the molecular diagnostics assays, revealed colocalizations of three intra-host SNVs and 2 isolate-specific SNVs with primers and probes currently in use. In detail, intra-host SNVs colocalized with the probe of RdRP\_SARSr reaction (15,474 T > G), with the reverse primer of HKU-N reaction (28,971 A > G) and with the probe of 2019-nCoV-N2 reaction (29,095 T > C). More importantly, two SNVs belonging to isolates Wuhan/IVD-HB-04/2020 and Chongqing/YC01/2020, colocalized with the forward primer of 2019-nCoV-N1 reaction (28,291 C > T) and the probe of 2019nCoV-N2 reaction (29,200 C > T), respectively (**Figure 2**).

The *de novo* assembly of the viral genomes revealed intra-host genomic rearrangements. For samples SRR10903401 and SRR10903402, these large-scale structural events were systematically observed over poly-A / poly-U-rich genomic regions, located in ORF1ab and S genes. In all cases, similar or identical strings of nucleotides in close proximity appear to have served as seeds for homologous recombination events. All rearrangements were validated by remapping of the raw reads on the corresponding *de novo* assembled contigs, setting a threshold of at least 5 supporting reads of high mapping quality (>40) in each case. For sample SRR10903401 we isolated three inversions/misassemblies in ORF1ab (**Suppl. Figure 2**) and one inversion/misassembly in S gene (**Figure 3-A**). Notably, we were able to validate the same inversion in S gene for sample SRR10903402 as well (**Figure 3-B**). Apart from 2 inversions in ORF1ab supported by only 2 reads each (not passing the validation threshold), there were no further large-scale intra-host events observed for sample SRR10903402. Similarly, we identified one inversion/misassembly in sample SRR10971381 that was supported by only one read. The alignment coordinates of all rearrangement-supporting contigs with respect to the reference strain are presented in (**Table 2**).

## DISCUSSION

The rapid spread and the death toll of the new SARS-CoV-2 epidemic warrants the immediate identification / development of effective antiviral agents and vaccines, but also the design of accurate diagnostics. The intra- and inter- patient variability of the viral genome plays a pivotal role in all the abovementioned efforts, since it affects the compatibility of molecular diagnostics but also impairs the effectiveness of the vaccines and the serological assays by altering the antigenicity of the virus. Intra-host low-frequency variants are also the main source of resistance to anti-viral drugs.

Bioinformatics analysis of NGS data allows the generation of the consensus sequence of a viral genome from the of majority nucleotides at each position but also the identification of non-consensus nucleotides, enabling the exploration of intra-host variability but also its consequences on intra-host viral evolution [28]–[30]. All samples analysed in this study were probably infected by the same viral strain since they shared the same set of consensus SNVs. However, apart from 3 intra-host SNVs that were common between SRR10903401 and SRR10903402, there was no other overlap observed between the low frequency variants of each sample (**Figure 1-B**). This indicates that these variations have been occurred in a rather random fashion and are not subject of selective pressures, which is also supported by the fact that the missense mutations were systematically more, compared to the synonymous mutations. On the other hand, missense substitutions are more common in loci involving pathogen resistance, indicating positive selection [31]. The analysed viral RNA might have been originated from functional/packed virions, but also from unpacked viral genomes, which are unable to replicate and infect other host cells. Even if a viral genome is unable to replicate independently, its abundant presence in the pool of viral quasispecies implies some functionality regarding the intra-host evolution and adaptation. For example, defective viral genomes might affect infection dynamics such as viral persistence but also the natural history of an infection [32]–[34]. At the same time, these variants may arise rapidly during an outbreak and can be used for tracking the transmission chains and the spatiotemporal characteristics

of the epidemic [35]–[37]. Studies involving large number of samples and in-vitro experiments on SARS-CoV-2 viral isolates are needed, in order to conclude whether these variations are advantageous or come with a fitness cost for the virus.

SNVs and quasispecies that are observed at low frequency could represent viral variations of low impact on the functionality of the genome. However, their abundance is largely affected by the population size and the epidemic characteristics. For example, a neutral substitution in a region that represents a primer target for a molecular diagnostic assay can drift to fixation rather quickly in a rapidly spreading virus, jeopardizing the sensitivity of the assay [38], [39]. Here, we highlight three intra-host but also two fixed variants that colocalized with primers or probes of real-time PCR diagnostics assays that are currently in use (**Figure 2**). Since the alignment of these oligos with their genomic targets is directly linked to the performance of the corresponding diagnostic assays, the community should pay extra attention in the evaluation of these potentially emerging variations and be alerted, in case redesigning of these oligos is needed.

As it is well documented, recombination events lead to substantial changes in genetic diversity of RNA viruses [40], [41]. In CoVs, discontinuous RNA synthesis is commonly observed, resulting in high frequencies of homologous recombination [42], which can be up to 25% across the entire CoV genome [43]. For pathogenic HCoV genomic rearrangements are frequently reported during the course of epidemic outbreaks, such as HCoV-OC43 [44], and HCoV-NL63 [45], SARS-CoV [46][44] and MERS-CoV [47]. We have isolated intra-host genomic rearrangements, located in poly-A and poly-U enriched palindrome regions across the SARS-CoV-2 genome (**Figure 3, Suppl. Figure 1**). We have validated the majority of these events by visual inspection of the alignments. We conclude that these rearrangements do not represent artifacts derived from the NGS library preparation (e.g. PCR crosstalk artifacts), especially since all the supporting reads were not duplicated and, in some cases, differed in polymorphic positions (**Suppl. Figure 2**).

Recombination processes involving S gene particularly, have been reported for SARS- and SARS-like CoV but also for HCoV-OC43. In the case of sister species HCoV-NL63 and

HCoV-229E, recombination breakpoints are located near 3'- and 5'-end of the gene [1][47]. S is a trimeric protein, which is cleaved into two subunits, the globular N-terminal S1 and the C-terminal S2 [48]. The S1 subunit consists of a signal peptide and the NT and receptor binding (RB) domains, with the latter sharing only 40% amino acid identity with other SARS-related CoVs. Our analysis revealed that similarly to other genomic regions, the S1 subunit hosts many low-frequency SNVs, characterized by higher density compared to the rest of the S gene sequence (**Figure 1-E**). The S2 subunit is highly conserved, with 99% identity compared to human SARS-CoV and two bat SARS-like CoVs [9]. The S2 subunit consists of two fusion peptides (FP, IFP), followed by two heptad repeats (HR 1 and 2), the pretransmembrane domain (PTM), the transmembrane and the cytoplasmic domain (TM, CP) [48]. In S gene, the same rearrangement event has taken place in two samples analyzed in this study. This observation highlights a potential recombination hot-spot in S gene. The rearrangement that was common between the two samples of this study is located in nt24,000 of the 2019-nCoV genome, which corresponds to the ~200nt linking region between the fusion peptides FP and IFP (aa 812-813). Examining closely the secondary structure of the RNA genome around the breakpoints, we suggest a model where the palindromes 5'-UGGUUUU-3' and 5'-AAAACCAA-3', have served as donor-acceptor sequences during the recombination event, since they are both exposed in the single-stranded internal loops formed in a highly structured RNA pseudoknot (**Figure 3-C**). The RB domain of the S protein has been tested as a potential immunogen as it contains neutralization epitopes which appear to have a role in the induction of neutralizing antibodies [16], [49]. It should be mentioned though that S protein of SARS-CoV is the most divergent in all strains infecting humans [50], [51], as in both C and N-terminal domains variations arise rapidly, allowing immunological escape [52]. Our findings support that apart from these variations, the N-terminal region also hosts a recombination hot-spot, which together with the rest of the observed rearrangements, indicates the genomic instability of SARS-CoV-2 over poly-A and poly-U regions.

**Authors' contributions:** TK: Conceptualization; Data curation; Formal analysis; Methodology; Supervision; Validation; Visualization; Writing - original draft; Writing - review & editing. GP: Data curation; Formal analysis; Writing - original draft; Writing - review & editing. MB: Visualization; Writing - review & editing. AM, ST and AM: Writing - original draft; Writing - review & editing.

**Ethics approval and consent to participate:** Not applicable.

**Declarations of interest:** None.

## FIGURE LEGENTS

**Figure 1:** Intra – host SNVs: (A) Intra host SNV frequency vs read depth in the corresponding alignment position (B) SNVs overlaps between the samples analysed (C) Intra-host SNVs frequency vs. variant type – synonymous, missense, nonsense (low, moderate, high impact respectively). (D) Intra-host SNVs frequency vs. all seven genes affected (ORF1ab, S, ORF3a, ORF6, ORF7a, ORF8, N). Average values are in red rhombs. (E) Density histogram of intra-host SNVs across the SARS-CoV-2 genome.

**Figure 2:** Truncated map of SARS-CoV-2 genome illustrating a subset of intra-host (blue lines) and globally collected, strain-specific SNVs (orange lines) with respect to the genomic targets of molecular diagnostics assays (red arrows – primers, red bars - probes). Three intra-host variants (orange triangles), and two strain specific variants (Wuhan/IVD-HB-04/2020 and Chongqing/YC01/2020 - red triangles), are colocalized with RdRP\_SARSr probe (15,474 T > G), HKU-N primer (28,971 A > G) and 2019-nCoV-N2 probe (29,095 T > C).

**Figure 3:** Recombination events in S gene. Samples SRR10903401 (A) and SRR10903402 (B). Alignments of the de novo assembled contigs with respect to the reference genome (MN 975262). Donor – acceptor palindrome sequences are indicated in green bars. Raw, non-duplicated NGS reads, validating the recombination event, are represented below the corresponding contig. (C): Prediction of the secondary structure of the genomic region spanning the rearrangement breakpoint (100 bases upstream and 100 bases downstream). The

corresponding donor- acceptor sequences, exposed in internal loops, are indicated in green bars.

## REFERENCES

- [1] V. M. Corman, D. Muth, D. Niemeyer, and C. Drosten, "Hosts and Sources of Endemic Human Coronaviruses," vol. 100, pp. 163–188, 2018, doi: 10.1016/bs.aivir.2018.01.001.
- [2] A. R. Fehr and S. Perlman, "HHS Public Access," pp. 1–23, 2016, doi: 10.1007/978-1-4939-2438-7.
- [3] D. Vijaykrishna, G. J. D. Smith, J. X. Zhang, J. S. M. Peiris, H. Chen, and Y. Guan, "Evolutionary Insights into the Ecology of Coronaviruses," *J. Virol.*, vol. 81, no. 8, pp. 4012–4020, 2007, doi: 10.1128/jvi.02605-06.
- [4] C. I. Paules, "Coronavirus Infections — More Than Just the Common Cold," vol. 2520, pp. 3–4, 2020, doi: 10.1007/82.
- [5] F. Li, W. Li, M. Farzan, and S. C. Harrison, "Structural biology: Structure of SARS coronavirus spike receptor-binding domain complexed with receptor," *Science (80-. )*, vol. 309, no. 5742, pp. 1864–1868, 2005, doi: 10.1126/science.1116480.
- [6] J. Cui, "Origin and evolution of pathogenic coronaviruses," *Nat. Rev. Microbiol.*, vol. 17, no. March, pp. 181–192, 2019, doi: 10.1038/s41579-018-0118-9.
- [7] J. H. Epstein *et al.*, "Bats Are Natural Reservoirs of SARS-Like Coronaviruses," *Science (80-. )*, vol. 310, no. 5748, pp. 676–679, 2005, doi: 10.1109/NEMS.2006.334722.
- [8] "Novel coronavirus 2019-nCoV: early estimation of epidemiological parameters and epidemic predictions," vol. 2020, no. January, 2020.
- [9] J. F. Chan *et al.*, "Genomic characterization of the 2019 novel human-pathogenic coronavirus isolated from a patient with atypical pneumonia after visiting Wuhan," vol. 1751, 2020, doi: 10.1080/22221751.2020.1719902.
- [10] B. Li *et al.*, "Rapid Reversion of Sequence Polymorphisms Dominates Early Human Immunodeficiency Virus Type 1 Evolution," *J. Virol.*, vol. 81, no. 1, pp. 193–201, 2007, doi: 10.1128/jvi.01231-06.
- [11] A. Beloukas *et al.*, "Assessment of phylogenetic sensitivity for reconstructing HIV-1 epidemiological relationships," *Virus Res.*, vol. 166, no. 1–2, pp. 54–60, 2012.
- [12] M. Vignuzzi, J. K. Stone, J. J. Arnold, C. E. Cameron, and R. Andino, "Quasispecies diversity determines pathogenesis through cooperative interactions in a viral population," *Nature*, vol. 439, no. 7074, pp. 344–348, 2006, doi: 10.1038/nature04388.
- [13] T. Karamitros *et al.*, "The interferon receptor-1 promoter polymorphisms affect the outcome of Caucasians with HB eAg-negative chronic HBV infection," *Liver Int.*, vol. 35, no. 12, pp. 2506–2513, 2015.
- [14] R. Malley, K. Trzcinski, A. Srivastava, C. M. Thompson, P. W. Anderson, and M.

- Lipsitch, "CD4+ T cells mediate antibody-independent acquired immunity to pneumococcal colonization," *Proc. Natl. Acad. Sci. U. S. A.*, vol. 102, no. 13, pp. 4848–4853, 2005, doi: 10.1073/pnas.0501254102.
- [15] M. Lipsitch and J. J. O'Hagan, "Patterns of antigenic diversity and the mechanisms that maintain them," *J. R. Soc. Interface*, vol. 4, no. 16, pp. 787–802, 2007, doi: 10.1098/rsif.2007.0229.
- [16] C. Y. Yong, H. K. Ong, S. K. Yeap, K. L. Ho, and W. S. Tan, "Recent Advances in the Vaccine Development Against Middle East Respiratory Syndrome-Coronavirus," *Front. Microbiol.*, vol. 10, no. August, pp. 1–18, 2019, doi: 10.3389/fmicb.2019.01781.
- [17] R. J. Nicolas W. Cortes-Penfield, Barbara W. Trautner, "A decade after SARS: Strategies to control emerging coronaviruses," *Physiol. Behav.*, vol. 176, no. 5, pp. 139–148, 2017, doi: 10.1016/j.physbeh.2017.03.040.
- [18] B. Langmead and S. L. Salzberg, "Fast gapped-read alignment with Bowtie 2," *Nat. Methods*, vol. 9, no. 4, pp. 357–359, Apr. 2012, doi: 10.1038/nmeth.1923.
- [19] J. T. Robinson, H. Thorvaldsdóttir, A. M. Wenger, A. Zehir, and J. P. Mesirov, "Variant review with the integrative genomics viewer," *Cancer Research*, vol. 77, no. 21. American Association for Cancer Research Inc., pp. e31–e34, 01-Nov-2017, doi: 10.1158/0008-5472.CAN-17-0337.
- [20] H. Li *et al.*, "The Sequence Alignment/Map format and SAMtools," *Bioinformatics*, vol. 25, no. 16, pp. 2078–2079, Aug. 2009, doi: 10.1093/bioinformatics/btp352.
- [21] A. Wilm *et al.*, "LoFreq: A sequence-quality aware, ultra-sensitive variant caller for uncovering cell-population heterogeneity from high-throughput sequencing datasets," *Nucleic Acids Res.*, vol. 40, no. 22, pp. 11189–11201, Dec. 2012, doi: 10.1093/nar/gks918.
- [22] P. Cingolani *et al.*, "A program for annotating and predicting the effects of single nucleotide polymorphisms, SnpEff: SNPs in the genome of *Drosophila melanogaster* strain w1118; iso-2; iso-3," *Fly (Austin)*, vol. 6, no. 2, pp. 80–92, 2012, doi: 10.4161/fly.19695.
- [23] P. Cingolani *et al.*, "Using *Drosophila melanogaster* as a model for genotoxic chemical mutational studies with a new program, SnpSift," *Front. Genet.*, vol. 3, no. MAR, 2012, doi: 10.3389/fgene.2012.00035.
- [24] V. M. Corman *et al.*, "Detection of 2019 novel coronavirus (2019-nCoV) by real-time RT-PCR," *Euro Surveill.*, vol. 25, no. 3, Jan. 2020, doi: 10.2807/1560-7917.ES.2020.25.3.2000045.
- [25] A. Bankevich *et al.*, "SPAdes: A new genome assembly algorithm and its applications to single-cell sequencing," *J. Comput. Biol.*, vol. 19, no. 5, pp. 455–477, May 2012, doi: 10.1089/cmb.2012.0021.

- [26] S. F. Altschul, W. Gish, W. Miller, E. W. Myers, and D. J. Lipman, "Basic local alignment search tool," *J. Mol. Biol.*, vol. 215, no. 3, pp. 403–410, Oct. 1990, doi: 10.1016/S0022-2836(05)80360-2.
- [27] A. R. Gruber, R. Lorenz, S. H. Bernhart, R. Neuböck, and I. L. Hofacker, "The Vienna RNA websuite.," *Nucleic Acids Res.*, vol. 36, no. Web Server issue, p. W70, 2008, doi: 10.1093/nar/gkn188.
- [28] M. Cotten *et al.*, "Full-genome deep sequencing and phylogenetic analysis of novel human betacoronavirus," *Emerg. Infect. Dis.*, vol. 19, no. 5, pp. 736–742, May 2013, doi: 10.3201/eid1905.130057.
- [29] B. L. Haagmans, A. C. Andeweg, and A. D. M. E. Osterhaus, "The Application of Genomics to Emerging Zoonotic Viral Diseases," *PLoS Pathog.*, vol. 5, no. 10, p. e1000557, Oct. 2009, doi: 10.1371/journal.ppat.1000557.
- [30] E.-G. Kostaki *et al.*, "Unravelling the history of hepatitis B virus genotypes A and D infection using a full-genome phylogenetic and phylogeographic approach," *Elife*, vol. 7, p. e36709, 2018.
- [31] D. N. Cooper and N. P. Group., *Nature encyclopedia of the human genome*. London; New York: Nature Pub. Group, 2003.
- [32] J. Aaskov, K. Buzacott, H. M. Thu, K. Lowry, and E. C. Holmes, "Long-term transmission of defective RNA viruses in humans and *Aedes* mosquitoes," *Science (80-. )*, vol. 311, no. 5758, pp. 236–238, Jan. 2006, doi: 10.1126/science.1115030.
- [33] P. Farci *et al.*, "The outcome of acute hepatitis C predicted by the evolution of the viral quasispecies," *Science (80-. )*, vol. 288, no. 5464, pp. 339–344, Apr. 2000, doi: 10.1126/science.288.5464.339.
- [34] E. Karamichali *et al.*, "HCV defective genomes promote persistent infection by modulating the viral life cycle," *Front. Microbiol.*, vol. 9, p. 2942, 2018.
- [35] G. Magiorkinis *et al.*, "HIV-1 epidemic in Russia: an evolutionary epidemiology analysis," *Lancet*, vol. 383, p. S71, 2014.
- [36] D. Paraskevis *et al.*, "Molecular investigation of HIV-1 cross-group transmissions during an outbreak among people who inject drugs (2011--2014) in Athens, Greece," *Infect. Genet. Evol.*, vol. 62, pp. 11–16, 2018.
- [37] G. Magiorkinis *et al.*, "An innovative study design to assess the community effect of interventions to mitigate HIV epidemics using transmission-chain phylodynamics," *Am. J. Epidemiol.*, vol. 187, no. 12, pp. 2615–2622, 2018.
- [38] J. Y. Noh *et al.*, "Simultaneous detection of severe acute respiratory syndrome, Middle East respiratory syndrome, and related bat coronaviruses by real-time reverse transcription PCR.," *Arch. Virol.*, vol. 162, no. 6, pp. 1617–1623, Jun. 2017, doi: 10.1007/s00705-017-3281-9.

- [39] T. Karamitros *et al.*, “A contaminant-free assessment of Endogenous Retroviral RNA in human plasma.,” *Nat. Sci. Reports*, vol. 6, p. 33598, 2016.
- [40] E. C. Holmes, *The evolution and emergence of RNA viruses*. Oxford University Press, 2009.
- [41] E.-G. Kostaki *et al.*, “Spatiotemporal characteristics of the HIV-1 CRF02\_AG/CRF63\_02A1 epidemic in Russia and Central Asia,” *AIDS Res. Hum. Retroviruses*, vol. 34, no. 5, pp. 415–420, 2018.
- [42] M. M. C. Lai, “RNA recombination in animal and plant viruses,” *Microbiological Reviews*, vol. 56, no. 1. pp. 61–79, 1992, doi: 10.1128/membr.56.1.61-79.1992.
- [43] R. S. Baric, K. Fu, M. C. Schaad, and S. A. Stohlman, “Establishing a genetic recombination map for murine coronavirus strain A59 complementation groups,” *Virology*, vol. 177, no. 2, pp. 646–656, Aug. 1990, doi: 10.1016/0042-6822(90)90530-5.
- [44] S. K. P. Lau *et al.*, “Molecular Epidemiology of Human Coronavirus OC43 Reveals Evolution of Different Genotypes over Time and Recent Emergence of a Novel Genotype due to Natural Recombination,” *J. Virol.*, vol. 85, no. 21, pp. 11325–11337, Nov. 2011, doi: 10.1128/jvi.05512-11.
- [45] K. Pyrc *et al.*, “Mosaic Structure of Human Coronavirus NL63, One Thousand Years of Evolution,” *J. Mol. Biol.*, vol. 364, no. 5, pp. 964–973, Dec. 2006, doi: 10.1016/j.jmb.2006.09.074.
- [46] C.-C. Hon *et al.*, “Evidence of the Recombinant Origin of a Bat Severe Acute Respiratory Syndrome (SARS)-Like Coronavirus and Its Implications on the Direct Ancestor of SARS Coronavirus,” *J. Virol.*, vol. 82, no. 4, pp. 1819–1826, Feb. 2008, doi: 10.1128/jvi.01926-07.
- [47] J. S. M. Sabir *et al.*, “Co-circulation of three camel coronavirus species and recombination of MERS-CoVs in Saudi Arabia,” *Science (80-. )*, vol. 351, no. 6268, pp. 81–84, Jan. 2016, doi: 10.1126/science.aac8608.
- [48] G. Lu, Q. Wang, and G. F. Gao, “Bat-to-human: Spike features determining ‘host jump’ of coronaviruses SARS-CoV, MERS-CoV, and beyond,” *Trends Microbiol.*, vol. 23, no. 8, pp. 468–478, 2015, doi: 10.1016/j.tim.2015.06.003.
- [49] S. Agnihothram *et al.*, “Evaluation of serologic and antigenic relationships between middle eastern respiratory syndrome coronavirus and other coronaviruses to develop vaccine platforms for the rapid response to emerging coronaviruses,” *J. Infect. Dis.*, vol. 209, no. 7, pp. 995–1006, 2014, doi: 10.1093/infdis/jit609.
- [50] H. Bisht *et al.*, “Severe acute respiratory syndrome coronavirus spike protein expressed by attenuated vaccinia virus protectively immunizes mice,” *Proc. Natl. Acad. Sci. U. S. A.*, vol. 101, no. 17, pp. 6641–6646, Apr. 2004, doi:

10.1073/pnas.0401939101.

- [51] L. Enjuanes, M. L. DeDiego, E. Álvarez, D. Deming, T. Sheahan, and R. Baric, “Vaccines to prevent severe acute respiratory syndrome coronavirus-induced disease,” *Virus Res.*, vol. 133, no. 1, pp. 45–62, Apr. 2008, doi: 10.1016/j.virusres.2007.01.021.
- [52] L. Jiaming *et al.*, “The recombinant N-terminal domain of spike proteins is a potential vaccine against Middle East respiratory syndrome coronavirus (MERS-CoV) infection,” *Vaccine*, vol. 35, no. 1, pp. 10–18, Jan. 2017, doi: 10.1016/j.vaccine.2016.11.064.

## TABLES

**Table 1: Impact of Intra-host SNVs on viral genes**

Gene	Intra-host Variants, N			Total, N (v/kbgl)*
	Low (synonymous)	Moderate (missense)	High (stop gained)	
ORF1ab	19	53	2	74 (3.47)
S	6	9	1	16 (4.18)
ORF3a	0	1	0	1 (1.20)
E	0	0	0	0 (0)
M	0	0	0	0 (0)
ORF6	2	1	0	3 (16.21)
ORF7a	0	1	0	1 (2.73)
ORF8	0	3	0	3 (8.21)
N	2	4	0	6 (4.76)
ORF10	0	0	0	0 (0)
Total, N	29	72	3	

\*normalised variants per 1 kb gene length (variants / gene-length \*1000)

**Table 2: Alignment characteristics of de novo assembled contigs**

Contig Name	Contig Length	Reference* Coordinates		Contig Coordinates		Alignment Identity (%)	Alignment Type	Average Read Depth (x)	QC Pass#
		start	end	start	end				
<b>SRR10903401</b>									
Contig 1	23994	75	24068	23994	1	99.99	Correct	57.01	+
Contig 2	5681	24246	29891	1	5646	99.96	Correct	71.40	+
Contig 3	331	23992	24322	331	1	100	Correct	164.39	+
Contig 4	179	24221	24399	179	1	100	Correct	97.56	+
Contig 5	192	17816	17909	94	1	100	Inversion	7.22	+
		17933	18030	95	192	100	Correct		
Contig 6	181	18052	18152	101	1	100	Relocation, Inconsistency	8.12	+
		17766	17845	102	181	100	Misassembly		
Contig 7	169	1707	1765	62	4	100	Inversion	7.62	+
		1815	1903	63	151	97.75	Correct		
Contig 8	165	23992	24087	96	1	100	Inversion	18.04	+
		23963	24031	97	165	100	misassembly		
<b>SRR10903402</b>									
Contig 1	29842	133	29891	29842	84	99.98	Correct	234.32	+
Contig 2	242	2075	2139	178	242	100	Partial	1.09	-
Contig 3	242	21577	21629	242	190	100	Partial	1.06	-
Contig 4	173	23992	24090	102	4	100	Inversion	39.30	+
		23963	24033	103	173	100	Misassembly		
<b>SRR10971381</b>									
Contig 1	29902	1	29891	29897	7	99.98	Correct	267.59	+
Contig 2	241	516	559	163	120	100	Inversion	1.00	-
		472	501	119	90	100	Misassembly		

\* Corresponding to strain MN975262 coordinates

# contig supported by at least 5 non duplicated reads of mapping quality >40

# FIGURES

**Figure 1**

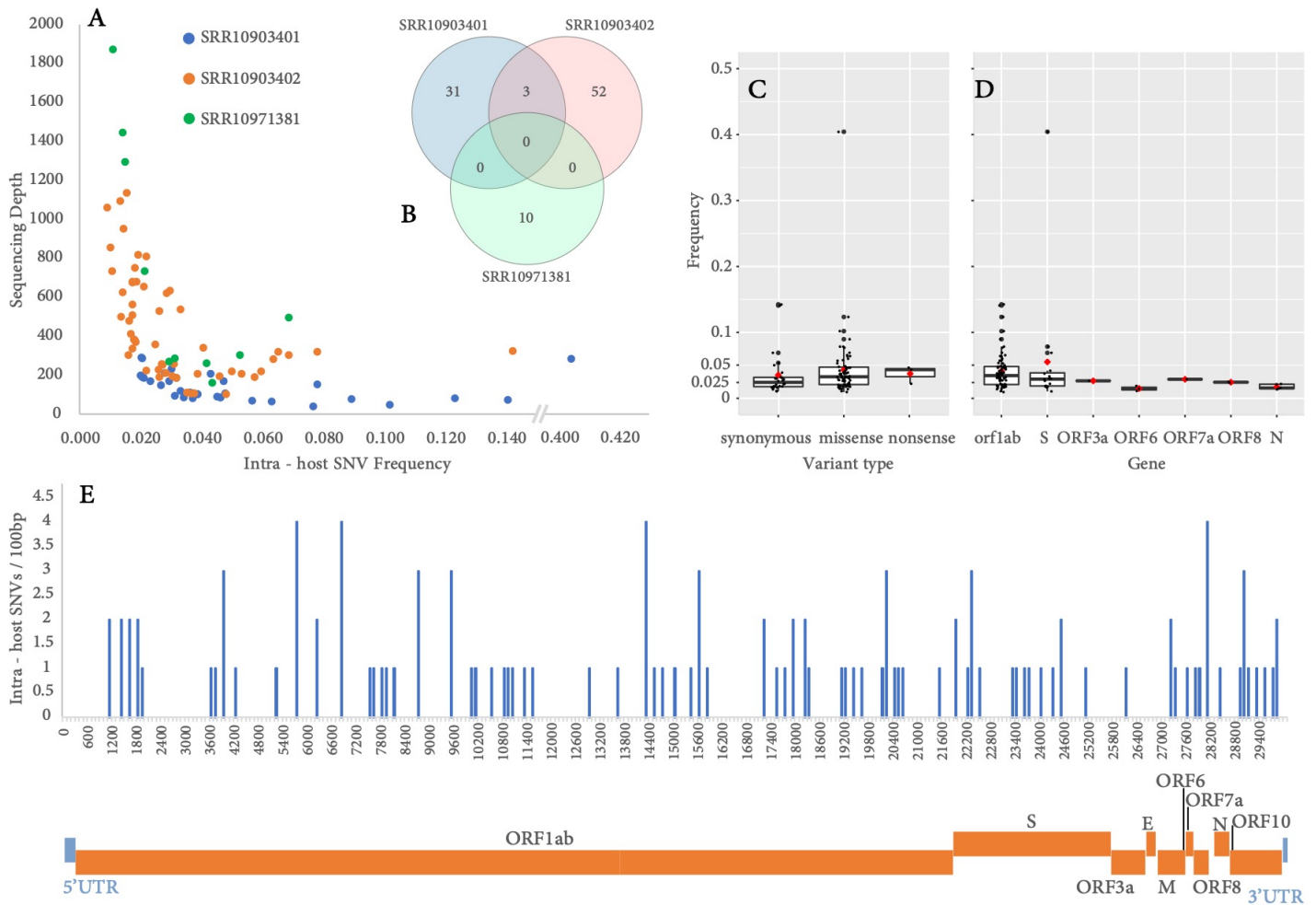


**Figure 1:** Intra – host SNVs: (A) Intra host SNV frequency vs read depth in the corresponding alignment position (B) SNVs overlaps between the samples analysed (C) Intra-host SNVs frequency vs. variant type – synonymous, missense, nonsense (low, moderate, high impact respectively). (D) Intra-host SNVs frequency vs. all seven genes affected (ORF1ab, S, ORF3a, ORF6, ORF7a, ORF8, N). Average values are in red rhombs. (E) Density histogram of intra-host SNVs across the SARS-CoV-2 genome.

**Figure 2**

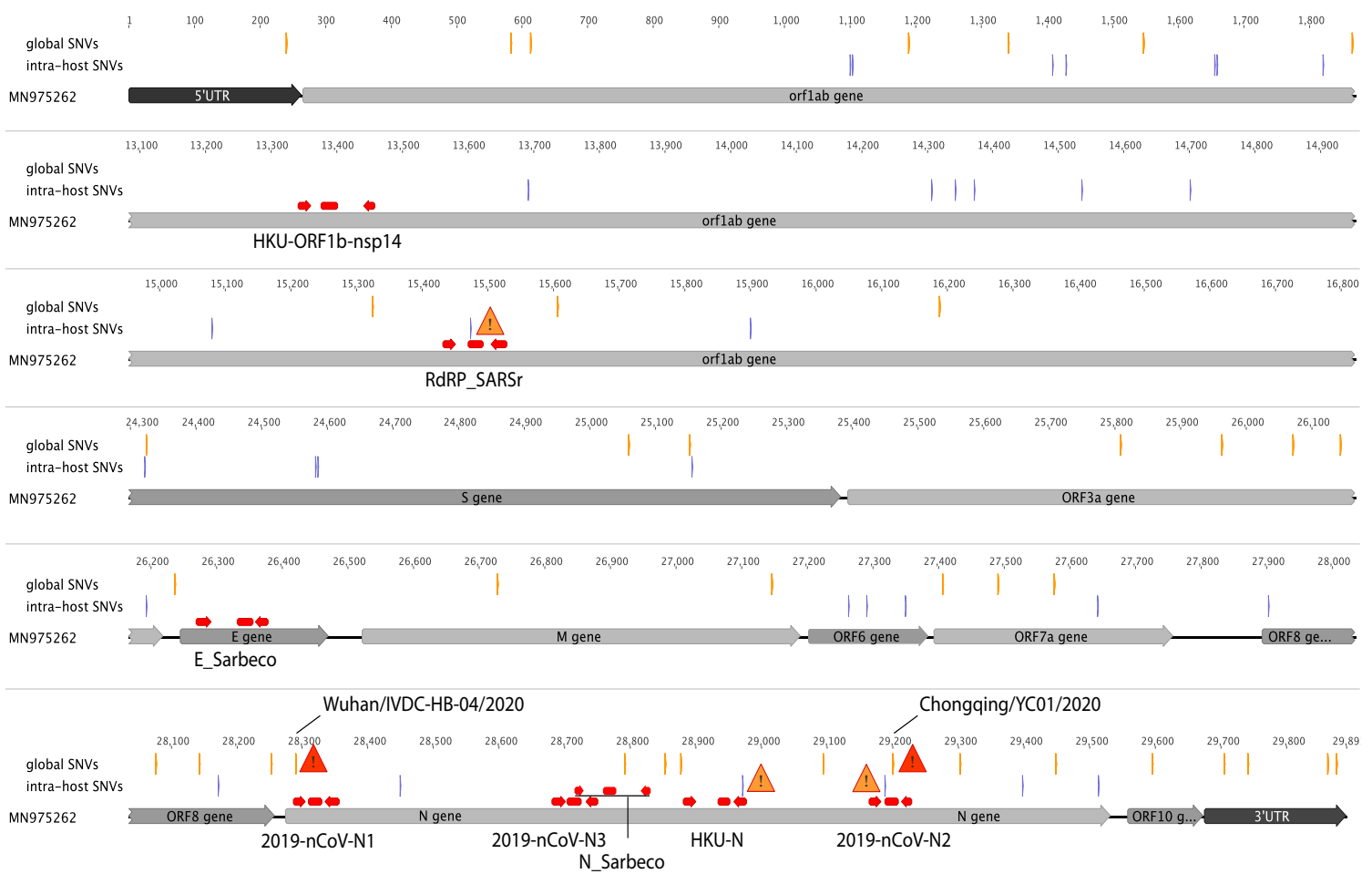


**Figure 2:** Truncated map of SARS-CoV-2 genome illustrating a subset of intra-host (blue lines) and globally collected, strain-specific SNVs (orange lines) with respect to the genomic targets of molecular diagnostics assays (red arrows – primers, red bars - probes). Three intra-host variants (orange triangles), and two strain specific variants (Wuhan/IVDC-HB-04/2020 and Chongqing/YC01/2020 - red triangles), are colocalized with RdRP\_SARSr probe (15,474 T > G), HKU-N primer (28,971 A > G) and 2019-nCoV-N2 probe (29,095 T > C).

**Figure 3**

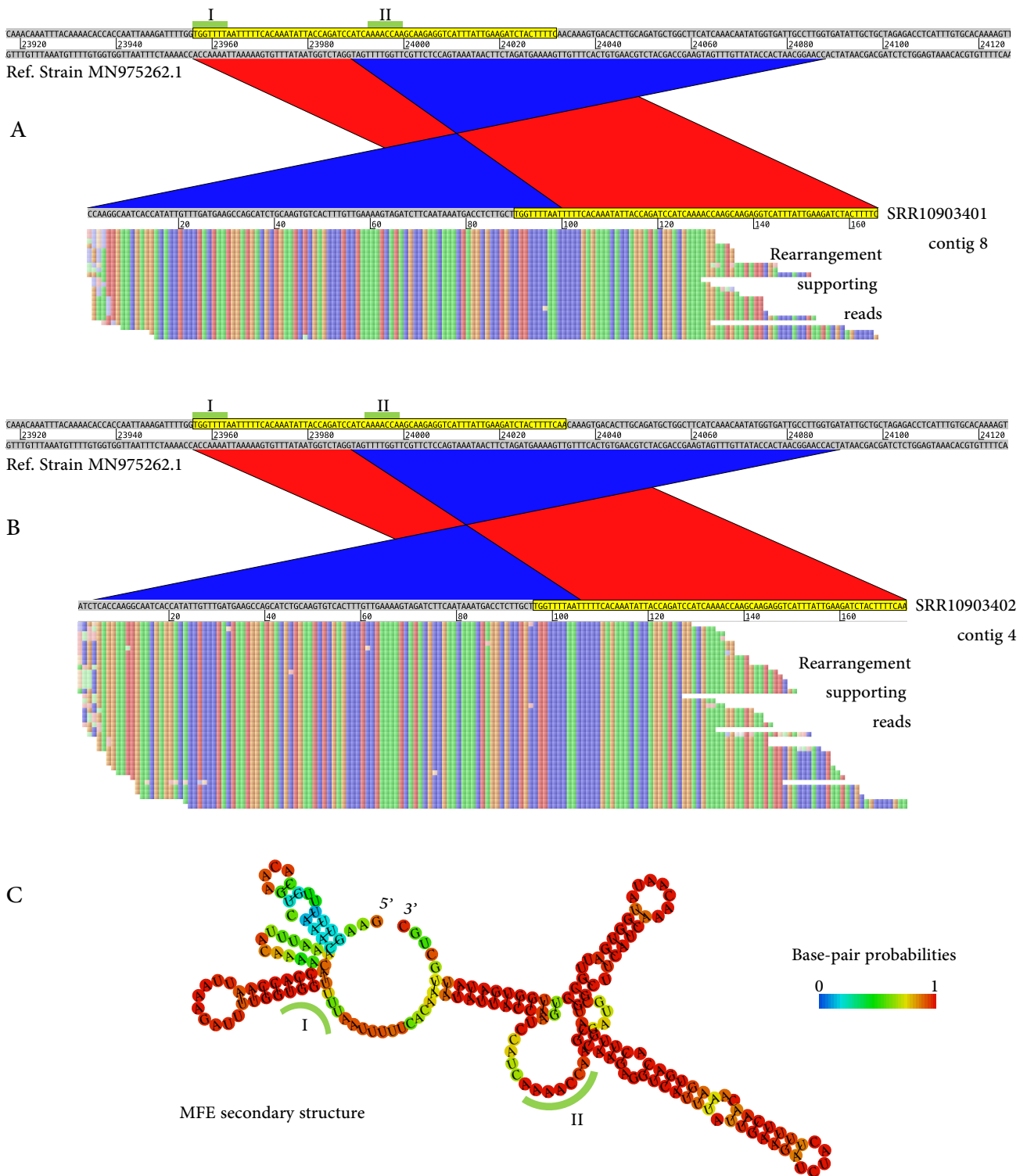


**Figure 3:** Recombination events in S gene. Samples SRR10903401 (A) and SRR10903402 (B). Alignments of the de novo assembled contigs with respect to the reference genome (MN 975262). Donor – acceptor palindrome sequences are indicated in green bars. Raw, non-duplicated NGS reads, validating the recombination

event, are represented below the corresponding contig. (C): Prediction of the secondary structure of the genomic region spanning the rearrangement breakpoint (100 bases upstream and 100 bases downstream). The corresponding donor-acceptor sequences, exposed in internal loops, are indicated in green bars.

## Supplementary Material

Suppl. Table 1: NGS read alignment statistics

	Sample		
	SRR10903401	SRR10903402	SRR10971381
Paired Reads N (%)			
Total Number	476,632 (100)	676,694 (100)	28,282,964 (100)
Aligned	13,913 (2.94)	54,723 (8.18)	62,288 (0.22)
Concordantly Aligned	11,469 (2.40)	44,176 (6.52)	59,261(0.21)
Discordantly Aligned	2444 (0.53)	10,547 (1.67)	3027 (0.01)
Single Mates N (%)			
Aligned	244 (0.03)	1308 (0.11)	294(0.001)
% Overall Alignment Rate	2.94	8.18	0.22

**Suppl. Table 2: Annotation of all isolated SNVs on the viral genome (MN975262)**

SRR10903401											
Position	Ref	Alt	Qual.	Filter Pass	Read Depth	Variant Frequency	Variant Type**	Variant Impact***	Gene	Nt Modification	AA Modification
1409	C	T	106	+	104	0.048	MS	M	ORF1ab	c.1144C>T	p.His382Tyr
1821	G	A	158	+	81	0.123	MS	M	ORF1ab	c.1556G>A	p.Gly519Asp
3695	C	T	75	+	147	0.027	SV	L	ORF1ab	c.3430C>T	p.Leu1144Leu
3917	A	G	67	+	86	0.047	MS	M	ORF1ab	c.3652A>G	p.Ser1218Gly
3920	A	T	68	+	86	0.047	SG	H	ORF1ab	c.3655A>T	p.Lys1219*
3921	A	T	67	+	88	0.045	MS	M	ORF1ab	c.3656A>T	p.Lys1219Ile
5210	G	T	113	+	78	0.090	MS	M	ORF1ab	c.4945G>T	p.Ala1649Ser
5702	C	T	172	+	207	0.043	SG	H	ORF1ab	c.5437C>T	p.Gln1813*
7694	T	C	71	+	119	0.034	MS	M	ORF1ab	c.7429T>C	p.Phe2477Leu
8782	T	C	2433	+	67	*1.000	SV	L	ORF1ab	c.8517T>C	p.Ser2839Ser
9561	T	C	1088	+	29	*1.000	MS	M	ORF1ab	c.9296T>C	p.Leu3099Ser
10145	T	C	79	+	106	0.038	MS	M	ORF1ab	c.9880T>C	p.Trp3294Arg
10552	A	G	70	+	168	0.030	SV	L	ORF1ab	c.10287A>G	p.Glu3429Glu
10817	G	A	74	+	63	0.063	MS	M	ORF1ab	c.10552G>A	p.Ala3518Thr
10967	T	C	60	+	95	0.032	MS	M	ORF1ab	c.10702T>C	p.Phe3568Leu
12972	A	G	65	+	102	0.039	MS	M	ORF1ab	c.12707A>G	p.Asn4236Ser
14537	T	C	61	+	87	0.034	MS	M	ORF1ab	c.14273T>C	p.Leu4758Pro
14701	G	A	63	+	39	0.077	MS	M	ORF1ab	c.14437G>A	p.Asp4813Asn
15080	C	A	120	+	49	0.102	MS	M	ORF1ab	c.14816C>A	p.Ala4939Asp
15607	C	T	3146	+	86	*0.988	SV	L	ORF1ab	c.15343C>T	p.Leu5115Leu
17271	A	G	62	+	187	0.021	SV	L	ORF1ab	c.17007A>G	p.Lys5669Lys
17300	A	G	62	+	191	0.021	MS	M	ORF1ab	c.17036A>G	p.Tyr5679Cys
17934	C	A	75	+	290	0.021	SV	L	ORF1ab	c.17670C>A	p.Thr5890Thr
17936	G	A	76	+	286	0.021	MS	M	ORF1ab	c.17672G>A	p.Arg5891Lys
18253	A	T	142	+	168	0.048	MS	M	ORF1ab	c.17989A>T	p.Met5997Leu
18376	A	G	62	+	196	0.020	MS	M	ORF1ab	c.18112A>G	p.Thr6038Ala
19164	C	T	223	+	71	0.141	SV	L	ORF1ab	c.18900C>T	p.Asp6300Asp
19229	T	C	73	+	70	0.057	MS	M	ORF1ab	c.18965T>C	p.Ile6322Thr
19623	T	G	73	+	102	0.039	MS	M	ORF1ab	c.19359T>G	p.Ser6453Arg
20636	A	G	68	+	109	0.037	MS	M	ORF1ab	c.20372A>G	p.Glu6791Gly
21510	A	T	113	+	187	0.032	MS	M	ORF1ab	c.21246A>T	p.Glu7082Asp
21959	T	C	62	+	80	0.038	MS	M	S	c.397T>C	p.Phe133Leu

22316	G	A	171	+	153	0.078	MS	M	S	c.754G>A	p.Gly252Ser
23310	A	G	93	+	212	0.028	MS	M	S	c.1748A>G	p.Glu583Gly
23725	T	A	66	+	230	0.030	MS	M	S	c.2163T>A	p.Ser721Arg
24323	A	C	3240	+	277	0.404	MS	M	S	c.2761A>C	p.Lys921Gln
28144	C	T	5965	+	160	*1.000	MS	M	ORF8	c.251C>T	p.Ser84Leu
28173	A	G	74	+	169	0.024	MS	M	ORF8	c.280A>G	p.Lys94Glu
29095	T	C	8458	+	231	*0.996	SV	L	N	c.822T>C	p.Phe274Phe
<b>SRR10903402</b>											
1101	C	T	224	+	319	0.078	MS	M	ORF1ab	c.836C>T	p.Ser279Phe
1104	T	A	189	+	320	0.066	MS	M	ORF1ab	c.839T>A	p.Ile280Lys
1429	T	C	68	+	479	0.017	SV	L	ORF1ab	c.1164T>C	p.His388His
1656	T	A	69	+	379	0.018	MS	M	ORF1ab	c.1391T>A	p.Val464Asp
1659	G	T	67	+	383	0.018	MS	M	ORF1ab	c.1394G>T	p.Gly465Val
1821	G	A	329	+	304	0.069	MS	M	ORF1ab	c.1556G>A	p.Gly519Asp
1927	T	C	80	+	228	0.026	SV	L	ORF1ab	c.1662T>C	p.Thr554Thr
3761	G	A	86	+	564	0.018	MS	M	ORF1ab	c.3496G>A	p.Val1166Ile
5710	A	G	139	+	752	0.019	SV	L	ORF1ab	c.5445A>G	p.Glu1815Glu
5765	G	A	89	+	680	0.018	MS	M	ORF1ab	c.5500G>A	p.Gly1834Ser
5766	G	C	87	+	674	0.018	MS	M	ORF1ab	c.5501G>C	p.Gly1834Ala
6254	G	T	105	+	256	0.031	MS	M	ORF1ab	c.5989G>T	p.Ala1997Ser
6255	C	T	90	+	256	0.027	MS	M	ORF1ab	c.5990C>T	p.Ala1997Val
6810	T	C	65	+	112	0.036	MS	M	ORF1ab	c.6545T>C	p.Phe2182Ser
6813	C	G	71	+	108	0.037	MS	M	ORF1ab	c.6548C>G	p.Thr2183Ser
6816	G	A	65	+	105	0.038	MS	M	ORF1ab	c.6551G>A	p.Arg2184Lys
6828	C	G	84	+	103	0.049	MS	M	ORF1ab	c.6563C>G	p.Ser2188Cys
7541	A	C	220	+	341	0.041	MS	M	ORF1ab	c.7276A>C	p.Ile2426Leu
7854	A	G	72	+	624	0.014	MS	M	ORF1ab	c.7589A>G	p.Asn2530Ser
7970	A	T	89	+	1058	0.009	MS	M	ORF1ab	c.7705A>T	p.Ile2569Leu
8196	C	T	77	+	499	0.014	MS	M	ORF1ab	c.7931C>T	p.Ser2644Leu
8782	T	C	6957	+	201	*0.980	SV	L	ORF1ab	c.8517T>C	p.Ser2839Ser
9561	T	C	3842	+	105	*1.000	MS	M	ORF1ab	c.9296T>C	p.Leu3099Ser
10080	C	T	71	+	410	0.017	MS	M	ORF1ab	c.9815C>T	p.Pro3272Leu
11367	A	T	199	+	190	0.058	MS	M	ORF1ab	c.11102A>T	p.Tyr3701Phe
11563	C	T	1017	+	323	0.142	SV	L	ORF1ab	c.11298C>T	p.Cys3766Cys
13693	A	T	276	+	281	0.064	MS	M	ORF1ab	c.13429A>T	p.Thr4477Ser
14307	T	C	142	+	219	0.050	SV	L	ORF1ab	c.14043T>C	p.Tyr4681Tyr
14308	T	C	91	+	217	0.060	MS	M	ORF1ab	c.14044T>C	p.Trp4682Arg

14344	T	C	79	+	187	0.032	SV	L	ORF1ab	c.14080T>C	p.Leu4694Leu
14373	A	G	67	+	225	0.022	SV	L	ORF1ab	c.14109A>G	p.Ala4703Ala
15474	T	G	80	+	205	0.054	SV	L	ORF1ab	c.15210T>G	p.Gly5070Gly
15607	C	T	8759	+	238	*0.992	SV	L	ORF1ab	c.15343C>T	p.Leu5115Leu
15900	T	C	77	+	210	0.029	SV	L	ORF1ab	c.15636T>C	p.Val5212Val
17543	T	A	76	+	732	0.011	MS	M	ORF1ab	c.17279T>A	p.Met5760Lys
17737	A	G	168	+	819	0.020	MS	M	ORF1ab	c.17473A>G	p.Thr5825Ala
18253	A	T	189	+	634	0.030	MS	M	ORF1ab	c.17989A>T	p.Met5997Leu
19452	T	A	84	+	383	0.018	SV	L	ORF1ab	c.19188T>A	p.Ala6396Ala
20236	A	C	67	+	194	0.031	SV	L	ORF1ab	c.19972A>C	p.Arg6658Arg
20236	A	G	122	+	194	0.046	MS	M	ORF1ab	c.19972A>G	p.Arg6658Gly
20238	G	A	95	+	205	0.039	SV	L	ORF1ab	c.19974G>A	p.Arg6658Arg
20412	A	C	66	+	254	0.028	MS	M	ORF1ab	c.20148A>C	p.Glu6716Asp
21904	C	T	65	+	304	0.016	SV	L	S	c.342C>T	p.Thr114Thr
22270	T	C	124	+	509	0.018	SV	L	S	c.708T>C	p.Thr236Thr
22316	G	A	218	+	539	0.033	MS	M	S	c.754G>A	p.Gly252Ser
22326	C	T	157	+	528	0.027	MS	M	S	c.764C>T	p.Ser255Phe
23687	A	G	96	+	679	0.019	MS	M	S	c.2125A>G	p.Asn709Asp
24082	C	A	70	+	810	0.022	SG	H	S	c.2520C>A	p.Cys840*
24583	T	C	74	+	856	0.011	SV	L	S	c.3021T>C	p.Tyr1007Tyr
25156	C	T	79	+	336	0.018	SV	L	S	c.3594C>T	p.Ile1198Ile
26194	A	T	72	+	189	0.026	MS	M	ORF3a	c.802A>T	p.Thr268Ser
27292	T	C	80	+	370	0.019	MS	M	ORF6	c.91T>C	p.Tyr31His
27644	C	G	205	+	622	0.029	MS	M	ORF7a	c.251C>G	p.Pro84Arg
27904	T	A	70	+	357	0.025	MS	M	ORF8	c.11T>A	p.Leu4His
28144	C	T	19121	+	522	*1.000	MS	M	ORF8	c.251C>T	p.Ser84Leu
28971	A	G	99	+	1137	0.016	MS	M	N	c.698A>G	p.Lys233Arg
29095	T	C	34590	+	955	*0.996	SV	L	N	c.822T>C	p.Phe274Phe
29188	A	G	76	+	1093	0.014	SV	L	N	c.915A>G	p.Ala305Ala
29398	G	C	109	+	950	0.015	MS	M	N	c.1125G>C	p.Lys375Asn
29514	C	G	91	+	654	0.021	MS	M	N	c.1241C>G	p.Ala414Gly
<b>SRR10971381</b>											
4281	T	C	181	+	302	0.052	MS	M	ORF1ab	c.4016T>C	p.Val1339Ala
27264	T	C	76	+	1872	0.018	SV	L	ORF6	c.63T>C	p.Thr21Thr
27351	T	C	86	+	1446	0.014	SV	L	ORF6	c.150T>C	p.Ser50Ser
20104	C	T	92	+	1294	0.015	MS	M	ORF1ab	c.19840C>T	p.Leu6614Phe
28450	T	A	70	+	732	0.021	MS	M	N	c.177T>A	p.His59Gln

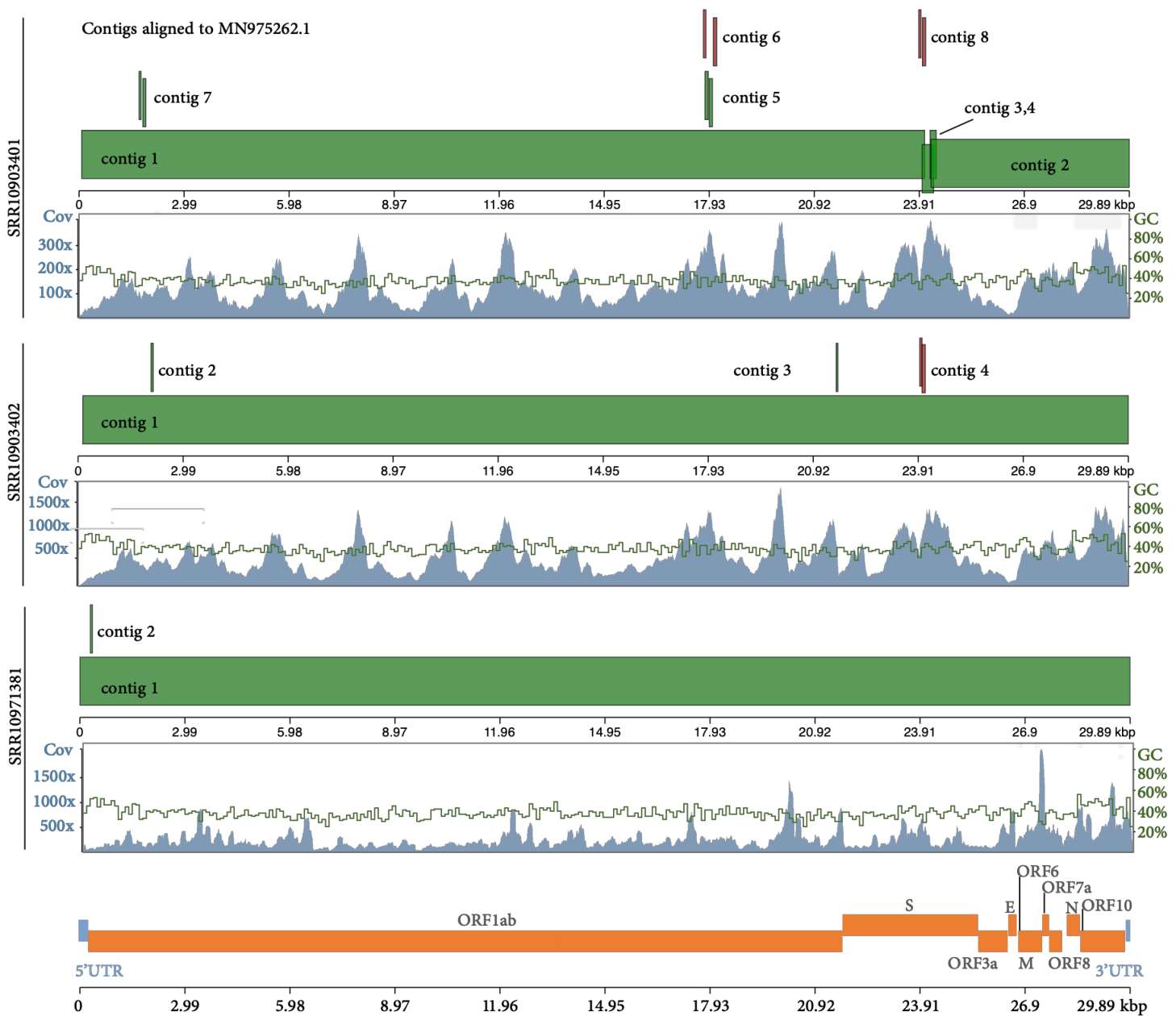
24586	G	C	81	+	268	0.029	SV	L	S	c.3024G>C	p.Val1008Val
20542	T	C	73	+	284	0.031	MS	M	ORF1ab	c.20278T>C	p.Ser6760Pro
22592	G	A	88	+	262	0.041	MS	M	S	c.1030G>A	p.Ala344Thr
11049	T	C	71	+	159	0.044	MS	M	ORF1ab	c.10784T>C	p.Val3595Ala
23434	T	C	341	+	493	0.068	SV	L	S	c.1872T>C	p.Ile624Ile

\*Variants with >98% frequency were excluded from downstream analysis of low-frequency variants.

\*\* Variant Type: MS=missense, SV=synonymous variant, SG= stop gained

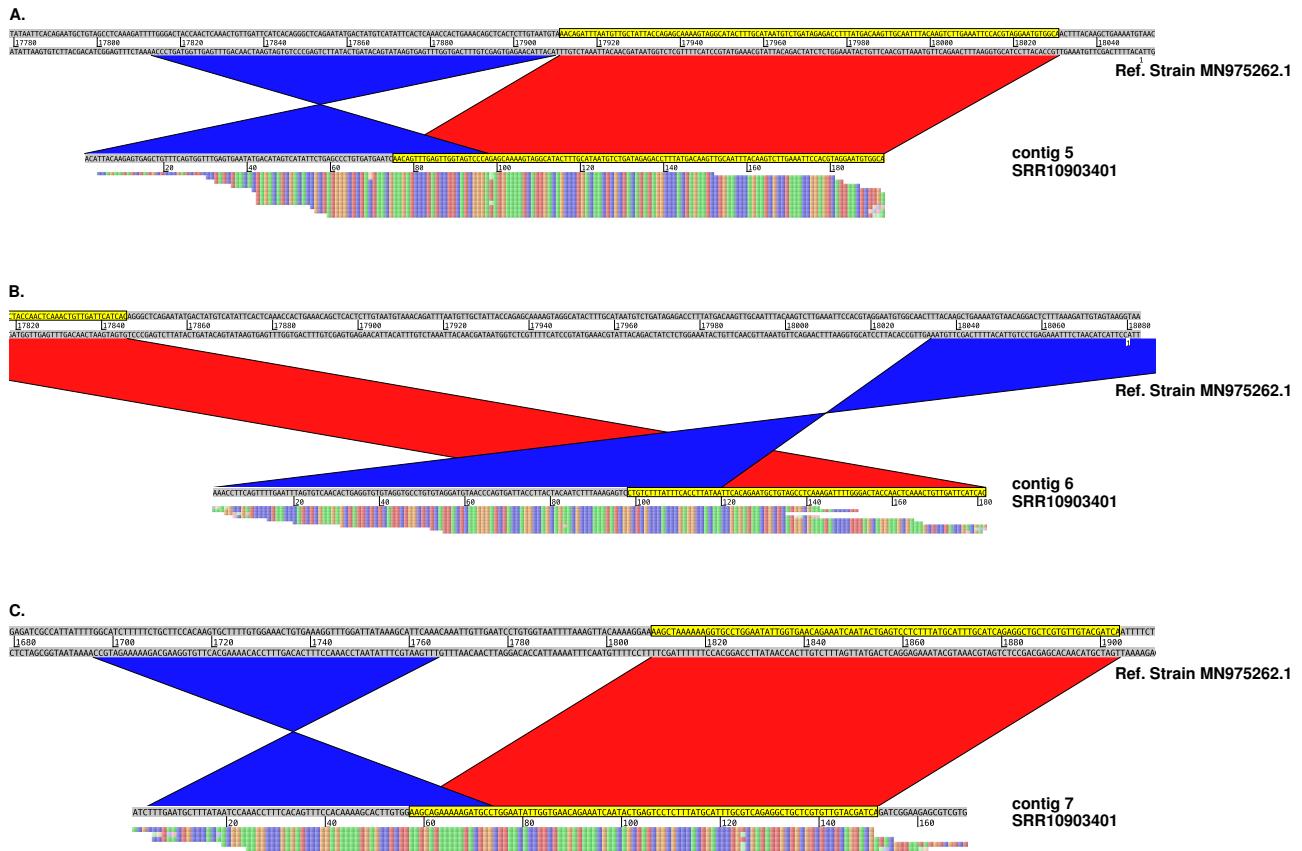
\*\*\*Variant Impact: L=low, M=moderate, H=high

## Suppl. Figure 1



**Suppl. Figure 1:** Alignment of the de novo assembled contigs on the genomic map (bottom). Concordantly aligned contigs (correct or gapped) are in green, while discordantly aligned are in red. Read depth plot (coverage) across the genome (blue) and relative % GC content (green) is presented for each sample.

## Suppl. Figure 2



**Suppl. Figure 2:** Recombination events in ORF1ab in sample SRR10903401. Alignments of the de novo assembled contigs with respect to the reference genome (MN 975262). Raw, non-duplicated NGS reads, validating the recombination event, are represented below the corresponding contig.